Electron Spin Resonance Characterization of Liquid Ordered Phase of Detergent-Resistant Membranes from RBL-2H3 Cells

Mingtao Ge,* Kenneth A. Field,* Rajindra Aneja,# David Holowka,* Barbara Baird,* and Jack H. Freed*
*Department of Chemistry and Chemical Biology, Baker Laboratory, Cornell University, Ithaca, New York 14853, and #Nutrimed Biotech, Cornell University Research Park, 270–276 Langmuir Laboratory, Ithaca, New York 14850 USA

ABSTRACT The dynamic structure of detergent-resistant membranes (DRMs) isolated from RBL-2H3 cells was characterized using two different acyl chain spin-labeled phospholipids (5PC and 16PC), a headgroup labeled sphingomyelin (SM) analog (SD-Tempo) and a spin-labeled cholestane (CSL). It was shown, by comparison to dispersions of SM, dipalmitoylphosphatidylcholine (DPPC), and DPPC/cholesterol of molar ratio 1, that DRM contains a substantial amount of liquid ordered phase: 1) The rotational diffusion rates ($R_\perp$) of 16PC in DRM between −5°C and 45°C are nearly the same as those in molar ratio DPPC/Chol = 1 dispersions, and they are substantially greater than $R_\perp$ in pure DPPC dispersions in the gel phase studied above 20°C; 2) The order parameters (S) of 16PC in DRM at temperatures above 4°C are comparable to those in DPPC/Chol = 1 dispersions, but are greater than those in DPPC dispersions in both the gel and liquid crystalline phases. 3) Similarly, $R_\perp$ for 5PC and CSL in DRM is greater than in pure SM dispersions in the gel phase, and S for these labels in DRM is greater than in the SM dispersions in both the gel and liquid crystalline phases. 4) $R_\perp$ of SD-Tempo in DRM is greater than in dispersions of SM in both gel and liquid phases, consistent with the liquid-like mobility in the acyl chain region in DRM. However, S of SD-Tempo in DRM is substantially less than that of this spin label in SM in gel and liquid crystalline phases (in absolute values), indicating that the headgroup region in DRMs is less ordered than in pure SM. These results support the hypothesis that plasma membranes contain DRM domains with a liquid ordered phase that may coexist with a liquid crystalline phase. There also appears to be a coexisting region in DRMs in which the chain labels 16PC and 5PC are found to cluster. We suggest that other biological membranes containing high concentrations of cholesterol also contain a liquid ordered phase.

INTRODUCTION

IgE receptors (FcεRI) initiate signaling in RBL-2H3 mast cells after aggregation by antigen. Recently, Field et al. (1997) showed that this process involves the association of these transmembrane receptors and the Src family protein-tyrosine kinase Lyn, which phosphorylates the β and γ subunits of FcεRI, with detergent-resistant membranes (DRMs) of a special composition. In addition, microscopy data show that the same interactions observed between aggregated IgE-FcεRI and DRM components after lysis at low concentrations of Triton X-100 (TX-100) also occur at the surface of intact cells (Pierini et al. 1996; Holowka et al., submitted for publication). These findings provide a structural basis for the initial coupling between Lyn and FcεRI in the cellular signaling process that utilizes stimulus-sensitive protein-lipid interactions. Recent evidence indicates that DRM-like structures, including morphologically identifiable caveolae, are involved in the signaling of other cell surface receptors (Anderson, 1998; Brown and London, 1998a) and in membrane trafficking (Simons and Ikonen, 1997).

Received for publication 8 December 1998 and in final form 30 April 1999.

Address reprint requests to Dr. Jack H. Freed, Department of Chemistry and Chemical Biology, Baker Laboratory, Cornell University, Ithaca, NY 14853-1301. Tel.: 607-255-3647; Fax: 607-255-0595; E-mail: jhf@msc.cornell.edu.

Dr. Field's present address is G. W. Hooper Foundation, University of California, San Francisco, CA 94143-0552.

0006-3495/99/08/925/09 $2.00

Elucidation of the molecular details of the mechanism by which these cellular signaling processes are initiated and promoted by DRM is a major challenge to both biochemists and biophysicists. Some progress has been made toward this goal by investigating the physical properties of these structures in model membranes. It is known that DRMs from cells are enriched in SM, gangliosides, and cholesterol (Chol) (Brown and Rose, 1992). Lund-Katz et al. (1988) showed that Chol packs more densely with sphingomyelin (SM) monolayers than with phosphatidylcholine (PC) monolayers. Recently, Schroeder et al. (1994) found that detergent-resistant liposomes with a composition similar to that of DRMs are as fluid as 1,2-dipalmitoylphosphatidylcholine/cholesterol (DPPC/Chol) membranes, which are known to be in a liquid ordered phase. The liquid ordered phase was defined by Ipsen et al. (1987) as the phase structure of model membranes containing a high concentration of Chol. Thus it was also referred to as a high-Chol liquid phase (Ipsen et al., 1987). Ahmed et al. (1997) further demonstrated that the formation of a liquid ordered phase is promoted by SM and Chol in model membranes, and they inferred that the detergent-insoluble membranes isolated from cells are likely to exist in the liquid ordered phase. Hanada et al. (1995) showed that both SM and Chol are involved in causing the insolubility of human placental alkaline phosphatase (a glycosylphosphatidylinositol (GPI)-linked protein) in TX-100, and they suggested that together, SM and Chol play a role in the formation of DRM. The role played by ganglioside GM_1 in DRMs was explored by

Ferroretto et al. (1997), who found that GM_1/SM, SM/Chol, and GM_1/GM_1 interactions all contribute to the formation of DRMs. Other recent studies show that the liquid ordered phase and not specific molecular interactions is responsible for the detergent insolubility of GPI-anchored proteins (Schroeder et al., 1998).

Despite these efforts, so far, no experimental results on the physical properties of DRMs directly isolated from cell membranes have been reported. Thus, for example, the question remains whether DRMs from cell membranes have a liquid ordered structure that could facilitate their phase segregation from the surrounding membranes. The mechanism of how DRMs are involved in the various biological processes is only partially understood (Sheets et al., 1999). We have conducted an electron spin resonance (ESR) spin-labeling study that characterizes the ordering and dynamics of DRM vesicles, isolated from RBL-2H3 cells after lysis by TX-100. Our results provide a detailed analysis of ESR spectra from a headgroup-labeled SM analog (SD-Tempo), two chain-labeled PCs (5PC and 16PC), and a spin-labeled Chol analog (CSL) incorporated into the DRM vesicles and vesicle dispersions of SM, DPPC, and DPPC/Chol = 1. By comparing the structural and dynamic properties of the DRM vesicles with these model membranes, and by comparing our ESR results with those from previous studies of the effects of Chol on the physical properties of model membranes, we find that the ordering and dynamics in DRM vesicles are very similar to those in dispersions of DPPC/Chol = 1 between 4°C and 45°C. We chose this concentration of Chol in the model membrane samples because the DPPC/Chol = 1 membrane is known to be in a liquid ordered phase (Brown and London, 1998b). Furthermore, the concentration of Chol in plasma membranes is known to be in the range of 30–50 mol% Chol (Gennis, 1989). In addition, this concentration of Chol is less than the maximum solubility of Chol in DPPC bilayers (Huang et al., 1999). Thus we confirm for the first time that the DRMs, derived from RBL-2H3 cell detergent lysates, contain the liquid ordered phase. We also find evidence for structural inhomogeneity in DRM, and this might play a role in IgE receptor signaling.

MATERIALS AND METHODS

Materials

Chain-labeled PCs (5PC and 16PC) and non-labeled lipids were purchased from Avanti (Alabaster, AL). The headgroup-labeled SM analog, SD-Tempo, was synthesized at Nutrimed Biotech (Ithaca, NY). The spin label 3β-doxyl-5α-cholestane (CSL), a Chol analogue, was purchased from Sigma Chemical Co. (St. Louis, MO). The chemical structures of these spin labels are shown in Fig. 1.

Sample preparations

Isolation of DRM from RBL-2H3 mast cells

RBL-2H3 cells were maintained in cell culture, harvested, and lysed in TX-100 as previously described (Field et al., 1995, 1997). For most experiments, 0.05% TX-100 (v/v) was used for lysis to produce conditions that preserve interactions with cross-linked IgE receptors (Field et al., 1997). For these, the lysates (4×10^6 cells/ml) were adjusted to 40% (wt/v) sucrose by diluting with an equal volume of 80% (wt/vol) sucrose for a final volume of 20 ml. The lysates were then layered with 5 ml each of 35% (w/v) and 5% (w/v) sucrose containing 25 mM Tris (pH 7.5), 125 mM NaCl, and 2 mM EDTA. Gradients were centrifuged in a SW27 rotor (Beckman Instruments, Palo Alto, CA) at 100,000 $\times$ *g* for 16 h at 4°C. The opaque material containing DRM vesicles at the interface of the 35% and 5% sucrose layers was harvested in ~3.0 ml. The DRM fractions from two or three identically prepared gradients were typically pooled before labeling. For experiments with CSL, 0.25% TX-100 (v/v) was used for cell lysis, and sucrose gradients of cell lysates were carried out as described by Field et al. (1995).

Incorporation of 16PC and 5PC into DRM vesicles

Pooled DRM fractions (6–9 ml) from sucrose gradients of cells ($8–10 \times 10^7$) lysed in 0.05% TX-100 (v/v) were diluted to 20 ml with 40 mM HEPES (pH 7.4) and centrifuged at 300,000 $\times$ *g* for 30 min in a Ti60 rotor

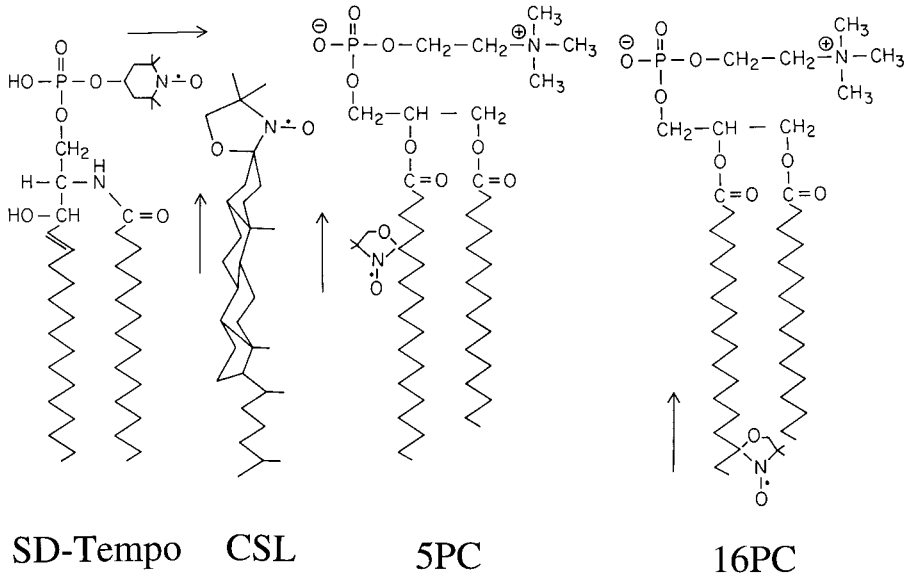

FIGURE 1 Chemical structures of spin labels SD-Tempo, CSL, 5PC, and 16PC. The arrows in each case show the principal axis of alignment in the membrane to which the motion of nitroxide moiety is sensitive. $R_\perp$ represents the rotational diffusion coefficient for the "wagging" motion of these axes.

(Beckman Instruments, Palo Alto, CA). Pelleted DRMs were resuspended in 1–3 ml of HEPES buffer (25 mM HEPES, pH 7.5, 150 mM NaCl, 2 mM EDTA). For each sample, 10–20 μl of 0.07 mM 16PC or 5PC in methanol was added dropwise to 1–2 ml of washed DRM, and methanol was added to a final concentration of 2% (v/v). Following incubation for 30 min to 2 h at 4°C, these samples were diluted to 4 ml with 25 mM HEPES buffer and centrifuged at 250,000 $\times$ g for 30 min in an SW60 rotor (Beckman Instruments). The DRM pellets were resuspended in 4 ml HEPES buffer and recentrifuged, and the pellets were transferred to a capillary of 1.5 mm internal diameter for ESR measurements. This amount of spin label was found to lead to optimal ESR spectra. Higher concentrations cause severe exchange broadening (cf. discussion below), whereas lower concentrations greatly reduce the signal-to-noise ratio.

Using Fourier transform mass spectrometry, it was determined that DRMs washed by centrifugation and resuspension as in the labeling procedure above contain no detectable TX-100 (i.e., <0.0001 (v/v)).

Incorporation of SD-Tempo into DRM vesicles

Eighty microliters of 0.03 mM SD-Tempo in methanol was added dropwise to DRM vesicles, which were pooled from sucrose gradients of cells (6–10 ml of 8–12 $\times$ 10^7 cell equivalents) lysed in 0.05% TX-100 as described above. Methanol was added to a final concentration of 2% (v/v), and the samples were incubated for 1 h at 4°C, then diluted to 4 ml in HEPES buffer. The labeled DRM vesicles were pelleted, washed, and analyzed as for DRM vesicles labeled with 16PC or 5PC described above. The amount of spin label used was found to optimize the ESR spectra (cf. above).

Incorporation of CSL into DRM vesicles

DRM vesicles prepared from $\sim$7 $\times$ 10^7 cells lysed in 0.25% TX-100 were recovered in 0.8 ml, and 30 μl of saturated CSL ($\sim$0.04 mM) in methanol was added to the DRM sample to optimize the ESR spectra as described above for SD-Tempo and the PC derivatives. DRM vesicles were then pelleted as described above. For some experiments, CSL-labeled DRM vesicles were washed by ultracentrifugation (250,000 $\times$ g for 10 min) and resuspended in 25 mM Tris (pH 7.5), 125 mM sodium chloride, and 2 mM EDTA, before a second ultracentrifugation and analysis of the pellet by ESR. Identical ESR spectra were obtained for pellets with and without the wash step.

Preparation of model membranes

Measured stock solutions of lipid (SM in chloroform:methanol 1:1 (v/v), and DPPC and chol in chloroform) and the spin label (SD-Tempo in chloroform:methanol 1:1 (v/v); other spin labels in chloroform) were mixed thoroughly in a glass tube. The total weight of dry lipids was 2 mg, and the concentration of spin labels was 0.5 mol% of the lipids for all samples except for the case of SD-Tempo, where it was 0.1 mol%. Additional experiments to check the effects of spin concentration were also performed. As the solvent was evaporated by N_2 flow, the dried lipids formed a thin film on the wall of the tube, then the sample was evacuated with a mechanical pump for at least 2 h to remove trace amounts of the solvent. After the addition of 2 ml of 50 mM Tris (pH 7.0), 160 mM sodium chloride, and 0.1 mM EDTA, the lipids were scraped off the wall, and the solution was stirred for 1 min and kept in the dark at room temperature for at least 2 h.

ESR spectroscopy and nonlinear least-squares analysis of ESR spectra

Spectra were obtained at a frequency of 9.55 GHz on a Bruker Instruments ER-200 ESR spectrometer equipped with a Varian temperature control unit. The field sweeps were calibrated with a Bruker ER 035M NMR gaussmeter. All spectra were digitized to 512 points and had $\sim$120G sweep widths. Nonlinear least-squares (NLLS) analyses of the spectra based on the stochastic Liouville equation (Meirovitch et al., 1982; Schneider and Freed, 1989) were performed using the latest fitting program (Budil et al., 1996), which yields the following parameters. $R_\perp$ is the rotational diffusion rate of the nitroxide radical around an axis perpendicular to the mean symmetry axis for the rotation. This symmetry axis is also the direction of preferential orientation of the spin-labeled molecule (Schneider and Freed, 1989). For 16PC and 5PC, $R_\perp$ represents the rotational wagging motion of the long axis of the acyl chains, whereas for CSL it is the rotational wagging motion of the long molecular axis (Ge et al., 1994). For the headgroup label SD-Tempo, it represents the rotational motion of the nitroxide headgroup (Ge and Freed, 1998). These are illustrated in Fig. 1. For the simulation of ESR spectra of spin labels incorporated into multilamellar vesicles, a MOMD model (which stands for microscopic order and macroscopic disorder; Meirovitch et al., 1984; Budil et al., 1996) was used. This model is based on the characteristics of the dynamic structure of lipid dispersions, i.e., locally in a lipid bilayer segment, lipid molecules are preferentially oriented by the structure of the bilayer, but globally the lipid bilayer segments are distributed randomly (Meirovitch et al., 1984). The order parameter, S, is a measure of the angular extent of the rotational diffusion of the nitroxide moiety; the larger S is, the more restricted is the motion. Therefore, S reflects the local ordering of lipid molecules in the disordered membrane dispersions. The magnetic A tensor and g tensor components needed for the simulations were obtained from fits to rigid limit spectra of the samples, which were taken at temperatures below -150°C.

RESULTS AND DISCUSSION

Comparison of DRM vesicles with SM, DPPC, and DPPC/Chol = 1 dispersions

ESR spectra from 16PC in DRM vesicles were collected from -5°C to 45°C; those in dispersions of pure DPPC were collected from 25°C to 50°C, which includes the temperature for the DPPC gel-to-liquid crystalline phase transition, 41°C (Marsh, 1990). Those in dispersions of DPPC/Chol = 1 were collected from -5°C to 50°C, to compare with the spectra from DRM vesicles and pure DPPC dispersions. Spectra (experimental and simulated) of 16PC at selected temperatures from DPPC, DPPC/Chol = 1 dispersions and DRM vesicles are shown in Fig. 2. All of

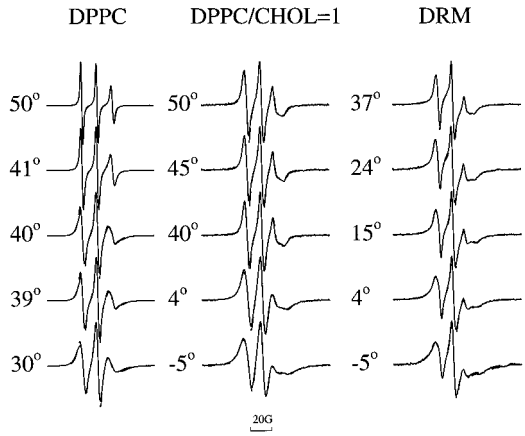

FIGURE 2 ESR spectra from spin label 16PC in dispersions of DPPC and DPPC/Chol = 1, and in DRM vesicles at selected temperatures (indicated in the figure). Solid lines, Experimental; dashed lines, simulated. (Due to good agreement, the dashed lines are barely visible).

the spectra from DPPC and DPPC/Chol = 1 dispersions can be simulated very well with just one component. However, the spectra from the DRM vesicles showed additional features characteristic of a broadened component. These spectra were simulated, allowing for two components in achieving the best least-squares fits. We find that one component is a spectrum with the normal three hyperfine lines, which is very similar to those obtained from the model membranes. The other spectrum is a single broad line, which is a clear indication of strong spin-spin interactions, which would be expected from clustering of the 16PC molecules (Fajer et al., 1992; Earle et al., 1994; and cf. below). The two components obtained from the simulation of the spectrum at 24°C are shown in Fig. 3. The relative population of the sharper component with three hyperfine lines is ~0.30 at all temperatures above −5°C, but it drops to 0.18 at −5°C. (Because the ESR signal height is inversely proportional to the square of the linewidth, we note that the broad component only makes a small contribution to the composite lineshape, as shown in Fig. 3.) The best fit parameters for $R_\perp$ and S of 16PC in the DRM vesicles and in dispersions of DPPC, DPPC/Chol = 1 are listed in Table 1, and their variations with temperature are shown in Fig. 4.

As shown in Fig. 4 *A* and Table 1, there is a sharp increase in $R_\perp$ of 16PC in DPPC dispersions from 40°C to 41°C, indicative of the gel-to-liquid crystalline (L_α) phase transition of DPPC bilayers. In contrast, the values of $R_\perp$ of 16PC in DRM vesicles increase smoothly from 8.71×10^7 s^{-1} at −5° to 3.22×10^8 s^{-1} at 45°C. They are greater than the values of $R_\perp$ of 16PC in DPPC dispersions of the gel phase, which are between 5.05×10^7 s^{-1} and 6.61×10^7 s^{-1}, and they are larger than or comparable to those in DPPC dispersions in the liquid crystalline phase, $1.00–4.00 \times 10^8$ s^{-1}. For DPPC/Chol = 1 dispersions, the values of $R_\perp$ are close to those for the DRM vesicles at the corresponding temperatures. Similarly, they show no sign of a gel-to-L_α phase transition.

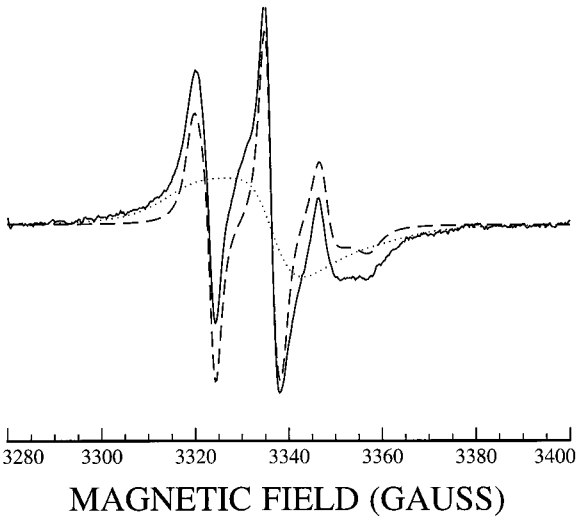

FIGURE 3 Two components (*dashed* and *dotted lines*) obtained from the NLLS fit for the ESR spectrum of 16PC in DRM vesicles at 24°C are superimposed on the experimental spectrum (*solid line*).

TABLE 1 Best fit parameters of $R_\perp$ and S from NLLS fits for ESR spectra of 16PC in dispersions of DPPC, DPPC/Chol═1 and in DRM vesicles

Sample	T (°C)	$R_\perp$ (s^{-1})	S	P
DPPC	25	6.62×10^7	0.16	—
	30	5.05×10^7	0.13	—
	35	5.92×10^7	0.07	—
	37	6.24×10^7	0.06	—
	39	6.61×10^7	0.06	—
	40	6.61×10^7	0.06	—
	41	1.03×10^8	0.00	—
	45	2.82×10^8	0.00	—
	50	4.06×10^8	0.00	—
DPPC/Chol═1	−5	6.17×10^7	0.16	—
	4	9.12×10^7	0.19	—
	15	1.48×10^8	0.22	—
	25	2.24×10^8	0.22	—
	30	2.51×10^8	0.22	—
	35	3.16×10^8	0.22	—
	40	3.31×10^8	0.22	—
	45	3.80×10^8	0.22	—
	50	4.07×10^8	0.21	—
DRM	−5	8.71×10^7	0.31	0.18
	4	9.77×10^7	0.26	0.33
	15	1.70×10^8	0.26	0.31
	24	2.34×10^8	0.23	0.26
	30	2.19×10^8	0.21	0.30
	37	2.57×10^8	0.20	0.31
	45	3.22×10^8	0.19	0.31

T = temperature; P = population of one component with normal three hyperfine line. The magnetic parameters used in the simulations are given as follows. 16PC in DPPC dispersions: $g_{xx} = 2.0089$, $g_{yy} = 2.0058$, $g_{zz} = 2.0021$; $A_{xx} = A_{yy} = 4.9$G, $A_{zz} = 33.0$G (from rigid limit spectra). 16PC in DPPC/Chol═1 dispersions: $g_{xx} = 2.0084$, $g_{yy} = 2.0054$, $g_{zz} = 2.0019$; $A_{xx} = A_{yy} = 5.0$G, $A_{zz} = 32.6$G (from rigid limit). 16PC in DRM vesicles: The g and A tensor components used are the same as those for 16PC in DPPC/Chol═1 dispersions. Least-squares estimated errors in $R_\perp$, ±5%; in S, ±0.01.

As shown in Fig. 4 *B* and Table 1, the curves of S versus temperature for DRM and for DPPC/Chol = 1 are comparable to each other above 4°C, with values of S that are significantly larger than those for DPPC dispersions in both its gel and L_α phases. It is also seen in Fig. 4 *B* that the value of S of 16PC in DPPC dispersions decreases from 0.16 at 25°C to 0.06 at 40°C, then drops to zero at 41°C, a further indication of the gel-to-L_α phase transition, with S becoming zero in the liquid crystalline phase. No such drop in S is observed in DRM vesicles, nor for DPPC/Chol = 1 dispersions over the whole temperature range studied.

The differences in the temperature dependence of $R_\perp$ and S for DRM and DPPC/Chol = 1 versus pure DPPC are consistent with the differences in their ESR lineshapes, as they must be. As shown in Fig. 2, when the temperature goes from 40°C to 41°C, the spectrum of 16PC in DPPC dispersions suddenly narrows. In contrast, over the wide temperature ranges studied, the spectra of 16PC in DRM vesicles and in DPPC/Chol = 1 dispersions change only gradually with temperature.

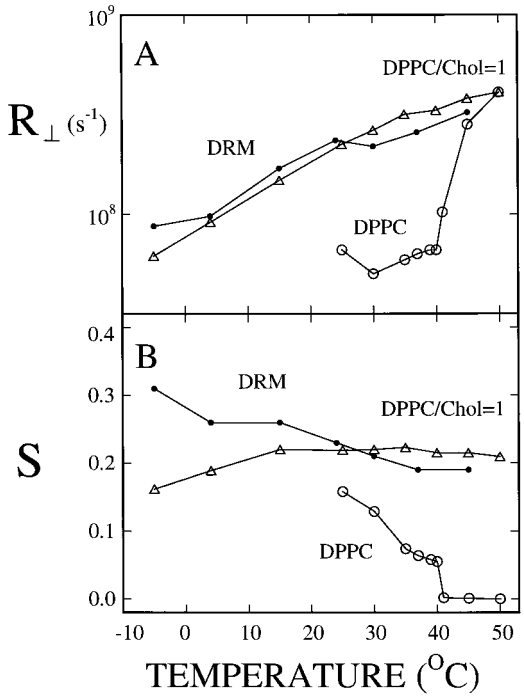

FIGURE 4 Variation of the rotational diffusion rate $R_\perp$ (*A*) and the order parameter *S* (*B*) of spin label 16PC with the temperature in dispersions of DPPC (○), DPPC/Chol = 1 (△), and DRM vesicles (●). The specific values of $R_\perp$ and *S* are tabulated in Table 1.

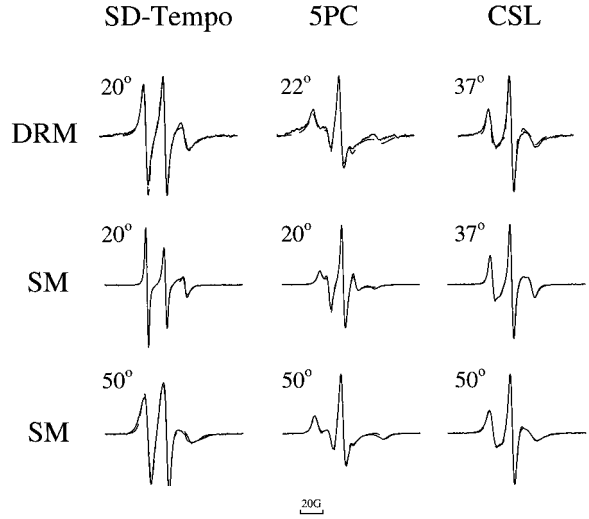

FIGURE 5 ESR spectra from spin labels SD-Tempo, 5PC, and CSL in DRM vesicles and SM dispersions. The temperatures (°C) for each spectrum are indicated in the figure. Solid lines, Experimental; dashed lines, simulated.

The above results with 16PC indicate that the physical properties of DRM vesicles are similar to those of DPPC/Chol = 1 dispersions and are quite different from those of DPPC dispersions. Specifically: 1) The ordering of the acyl chains near the center of the bilayers in DRM vesicles and in DPPC/Chol = 1 dispersions is higher than that in DPPC dispersions in the gel phase. 2) The rotational mobility of acyl chains near the center of the bilayers in DRM vesicles and in DPPC/Chol = 1 dispersions is comparable over the whole temperature range, but is significantly greater than that in pure DPPC dispersions in the gel phase (20–40°C); only in the L_α phase (>41°C) do the latter become comparable. 3) The characteristic gel-to-L_α phase transition at 41°C in DPPC dispersions is not observed in DPPC/Chol = 1 dispersions over the whole range of temperatures studied. Similarly, there is no sign of any phase transition for DRM vesicles in the corresponding temperature range.

We used additional spin labels to probe the dynamic structure over the acyl chain region and the headgroup region of the DRM: SD-Tempo, 5PC, and CSL. SD-Tempo is a good reporter of the headgroup region, 5PC is a good spin label for exploring the dynamic structure of acyl chains near the headgroup region, and CSL with its rigid molecular structure provides information about the overall dynamic and ordering properties of the acyl chain region (Kar et al., 1985; Tanaka and Freed, 1984). ESR spectra from these three spin labels in DRM vesicles at 20°C, 22°C, and 37°C are shown in Fig. 5 (experimental, *solid lines*; simulated, *dashed lines*). For purposes of comparison, ESR spectra from the same three spin labels in pure SM dispersions in the gel phase (20°C or 37°C) and in the L_α phase (50°C) are also shown in Fig. 5. The spectra from SD-Tempo and CSL in DRM were simulated using only one component. The spectrum from 5PC in DRM exhibited a broadening similar to that in the spectra from 16PC in DRM and was therefore simulated allowing for two components; again we found that one component has a normal three hyperfine pattern, and the other is just a single broad line. Relative populations of the two components are 0.28 and 0.72, respectively, which are close to those of the two components found from the simulations of the spectra from 16PC in the DRM vesicles.

The best fit parameters of $R_\perp$ and *S* from the NLLS analyses for the spectra in Fig. 5 are listed in Table 2. Note that SM and DPPC belong to sphingolipid and glycerophospholipid families, respectively. They are different in backbone structure, but the gel-to-L_α phase transition temperatures for SM with different N-acyl chain lengths (16–24) are 41–48°C (Marsh, 1990), and these are comparable to that for DPPC. Since SM is also an important component of DRMs (Fridriksson et al., 1999), we used it as an alternative model membrane system in our further comparisons with DRMs. From Table 2 it is seen that in DRM vesicles the value of *S* for 5PC at 22°C is 0.52, and for CSL at 37°C it is 0.85. These are even greater than those obtained in the gel phase of SM dispersions from 5PC at 20°C (0.46) and from CSL at 37°C (0.53), respectively. In addition, in DRM vesicles the values of $R_\perp$ of 5PC at 22°C, 4.07×10^7 s^{-1}, and of CSL at 37°C, 3.84×10^7 s^{-1}, are 2.5–4.6 times larger than those in the gel phase of SM dispersions at the corresponding temperatures. It is only in the L_α phase (50°C) that the $R_\perp$ of the two spin labels in the SM dispersions become comparable to those in the DRM at the lower

TABLE 2 Best fit parameters of $R_\perp$ and S from NLLS fits for ESR spectra of SD-Tempo, 5PC, and CSL in DRM vesicles and SM dispersions

S.L.	Sample	T (°C)	$R_\perp$ (s^{-1})	S
5PC*	DRM	22	4.07×10^7	0.52
	SM	20	1.62×10^7	0.46
	SM	50	7.08×10^7	0.37
CSL	DRM	37	3.84×10^7	0.85
	SM	37	8.31×10^6	0.53
	SM	50	2.43×10^7	0.49
SD-Tempo	DRM	20	4.15×10^7	0.06
	SM	20	5.00×10^6	0.32
	SM	50	2.82×10^7	−0.23

T = temperature; S.L. = spin label. The magnetic parameters used in the simulations are given as follows. SD-Tempo in DRM vesicles (from rigid limit spectra): $g_{xx} = 2.0084$, $g_{yy} = 2.0056$, $g_{zz} = 2.0020$; $A_{xx} = A_{yy} = 6.3$G, $A_{zz} = 36.0$G. SD-Tempo in SM dispersions (from rigid limit spectra): $g_{xx} = 2.0089$, $g_{yy} = 2.0053$, $g_{zz} = 2.0020$; $A_{xx} = A_{yy} = 5.6$G, $A_{zz} = 34.5$G. 5PC in SM/Chol═1 (from rigid limit spectra): $g_{xx} = 2.0086$, $g_{yy} = 2.0057$, $g_{zz} = 2.0015$; $A_{xx} = A_{yy} = 5.6$G, $A_{zz} = 34.8$G. The rigid limit spectrum of 5PC in DRM is not available because of the low signal-to-noise ratio, so the parameters for SM/Chol═1 were used. 5PC in SM dispersions (from rigid limit spectra): $g_{xx} = 2.0086$, $g_{yy} = 2.0057$, $g_{zz} = 2.0015$; $A_{xx} = A_{yy} = 5.6$G, $A_{zz} = 34.1$G. CSL in SM/Chol═1 (from rigid limit spectra): $g_{xx} = 2.0082$, $g_{yy} = 2.0057$, $g_{zz} = 2.0020$; $A_{xx} = A_{yy} = 6.5$G, $A_{zz} = 36.0$G. The rigid limit spectrum of CSL in DRM is not available because of the low signal-to-noise ratio, so the parameters for SM/Chol═1 were used. CSL in SM dispersions (from rigid limit spectra): $g_{xx} = 2.0082$, $g_{yy} = 2.0053$, $g_{zz} = 2.0018$; $A_{xx} = A_{yy} = 5.6$G, $A_{zz} = 34.1$G. Least-squares estimated errors in $R_\perp$ ±5%; in S, ± 0.02.

*The ESR spectrum of 5PC in DRM vesicles was fit with two components, a normal three hyperfine-line spectrum and a broad single line. The parameters listed in this table are for the first component. The Heisenberg exchange rate for 5PC for the broad component is 5.4×10^7 s^{-1}. The populations for the two components are 0.28 and 0.72, respectively.

temperatures; at the elevated temperatures, we would expect even larger values in the DRM, because $R_\perp$ increases significantly with temperature in all cases studied (cf. Fig. 4 and Shin and Freed, 1989a; Freed, 1994). These results from spin labels 5PC and CSL show that in the bilayers of DRM vesicles the acyl chains, either in the region near the headgroup or overall, are as ordered as in the gel (solid-like) phase of SM, but are as fluid as in the liquid crystalline (liquid-like) phase of SM. These results are consistent with those from 16PC presented above.

Molecular packing and interactions in the headgroup region have been explored less than in the acyl chain region. Recently we found that there is a strong orienting potential in the DPPC bilayer surface that is dependent on the phase structure of the bilayers (Ge and Freed, 1998). In our present study we have observed very similar behavior in SM bilayers, viz., we find that the change in order parameter of SD-Tempo in SM dispersions ranges from 0.32 at 20°C (gel phase) to −0.23 at 50°C (L_α phase) (see Table 2). The change in sign of S of SD-Tempo from positive to negative indicates that the nitroxide moeity changes its preferential orientation from perpendicular to parallel to the bilayer surface as SM dispersions go from the gel to the L_α phase. This type of behavior has previously been observed for another headgroup-labeled lipid in DPPC dispersions (Ge and Freed, 1998). These results show that there are strong interactions between lipid headgroups in the gel phase as well as in the liquid crystalline phase, but they exhibit different orienting properties. Table 2 shows that in DRM vesicles the order parameter S of SD-Tempo at 20°C, which is 0.06, is smaller in absolute value than for SM dispersions in either phase, indicating that the orienting potential at the surface of the DRM vesicles is weaker than in the bilayer surface of SM dispersions. In addition, Table 2 shows that the $R_\perp$ of SD-Tempo in DRM vesicles of 4.15×10^7 s^{-1} is faster than that in the L_α phase of SM, 2.82×10^7 s^{-1}. That is, the headgroup region in the DRMs is also more "fluid" than in the pure SM dispersions.

To summarize, the physical properties (ordering and dynamics of the bilayers) in DRM vesicles are very similar to those of DPPC/Chol = 1 dispersions, which are known to have a liquid ordered phase, but they are distinctly different from those of the pure lipid dispersions of DPPC and SM. It would thus appear that the DRM vesicles also have a liquid ordered phase. However, the chemical composition of the DRM vesicles is much more complex than that of the model systems. Recently it was shown by mass spectrometric analyses that DRM vesicles contain over 90 different species of SM, PC, phosphatidylethanolamine, phosphatidylserine, phosphatidylinositol, phosphatidylglycerol, and phosphatidic acid, with each class of lipids exhibiting a variety of different chain lengths and/or degrees of unsaturation (Fridriksson et al., 1999). Moreover, DRM vesicles contain Lyn and other membrane proteins. For such a complex system, one may ask to what extent its dynamic structure is affected by phospholipid/phospholipid and phospholipid/protein interactions, in addition to the phospholipid/Chol interactions. It would appear from the present study that, as far as the physical properties of the DRM vesicles are concerned, the lipid/Chol interactions dominate over all other lipid/lipid and lipid/protein interactions, such that the DRM vesicles and the DPPC/Chol = 1 dispersions have the same phase structure. (This statement applies to the DRM component that gives rise to the sharp line spectrum.) To examine this conclusion further, we next compare the properties that we found for the DRM with those of model membranes in the presence of high concentrations of Chol, as examined in previous studies.

Why are high concentrations of Chol essential for DRM?

Ipsen et al. (1987) defined the phase structure of model membranes containing high concentrations of Chol as a liquid ordered phase or, equivalently, as a high-cholesterol liquid phase. This definition was based on the two main effects of Chol on the structure and dynamics of lipid bilayers.

Ordering effect

Chol increases the acyl chain orientational ordering, which was observed by a variety of techniques, including ^{2}H NMR (Vist and Davis, 1990; Bloom et al., 1991), x-ray diffraction (McIntosh, 1978), fluorescence (Straume and Litman, 1987), and ESR (Kar et al., 1985; Shin and Freed, 1989a,b; Ge et al., 1994). Chol condenses the lipid monolayers at the air/water interface for both phosphoglycerol and sphingolipids (Bittman et al., 1994; Smaby et al., 1994, 1996). This effect is due to the strong van der Waals attractive interactions between the acyl chains and the planar rings of Chol, which reduces the number of *gauche* conformers of the acyl chains.

Fluidizing effect

Chol greatly increases both the acyl chain rotational mobility (Straume and Litman, 1987) and the lipid lateral mobility (Rubenstein et al., 1979) in the gel phase when the concentration of Chol is above 20–25 mol%. At high concentrations of Chol, the gel-to-L_α phase transition of lipid is abolished (Lewis and McElhaney, 1991), and the lipid bilayers remain in a fluid state over a wide range of temperatures (Vist and Davis, 1990). Another example of the fluidizing effect is that DMPC/Chol bilayers of molar ratio 1:1 have a very small surface rigidity, even at temperatures well below the DMPC L_α-to-gel phase transition, i.e., the bilayers behave like a surface liquid (Needham et al., 1988). The combined ordering and fluidizing effects of Chol were shown by ^{2}H NMR spectra obtained from chain deuterated lipids containing high concentrations of Chol. They are characteristic of a fluid lipid phase, yet the splittings are as large as in the gel phase (Bloom et al., 1991; Jacobs and Oldfield, 1979). Our ESR spectra, which provide both the order parameter and the rotational diffusional rate, show that even at -5°C DRM vesicles and DPPC/Chol = 1 dispersions have substantial $R_\perp$ but possess a solid-like ordering of the acyl chains. Furthermore, no phase transition in DRM vesicles and in DPPC/Chol = 1 dispersions could be detected.

For the headgroup region, strong interactions between headgroups were shown previously by nuclear Overhauser studies (Yeagle et al., 1975; 1977). In addition, it was shown (Yeagle et al., 1977) that Chol disrupts the molecular interactions between the headgroups. The spacer effect of Chol molecules was suggested as an explanation for the weakening of the interactions between headgroups (McIntosh et al., 1989). However, it seems that there is an additional effect of Chol. There was a significant increase in the surface dipole potential of egg PC monolayer when Chol was added until a PC-to-Chol molar ratio of 1:1 was reached (McIntosh et al., 1989). Furthermore, an increase in ordering of a fluorescent probe in the headgroup/water interface of a variety of PC vesicles was observed when 30 mol% of Chol was incorporated (Straume and Litman, 1987). These observations show that the structure of the lipid/water interface is altered by the incorporation of Chol. It was reported that there is a significant increase in the fluorescent probe depolarizing motion at the lipid/water interface in the presence of Chol (Straume and Litman, 1987). ESR (Tanaka et al., 1997) and dielectric relaxation (Henze, 1980) studies have shown that the motion of headgroups in PC dispersions is substantially increased upon incorporation of Chol. Our ESR observations of increased $R_\perp$ and reduced absolute values of S of SD-Tempo in DRM vesicles compared to the pure SM dispersions (see Table 2) are consistent with the enhanced motion of headgroups and the disrupted interactions between headgroups caused by the incorporation of Chol.

The above comparisons indicate that in both the acyl chain and headgroup regions the ordering and dynamics of DRM vesicles derived from RBL-2H3 cells are consistent with the characteristic properties of lipid bilayers containing high concentrations of Chol. In other words, lipid/Chol interactions do appear to dominate the molecular interactions in the DRM vesicles, consistent with DRM vesicles having a liquid ordered phase structure.

This conclusion can be further rationalized. As shown by Smaby et al. (1994), the requirement for a maximum Chol-induced condensation effect is that at least one hydrocarbon chain is long and capable of an extended conformation, which would ensure strong van der Waals attractive interactions with Chol's planar hard core. This requirement is not stringent. The 18C sphingosine base of SM satisfies this condition, because its 4,5 *trans* double bond is quite close to the interface region and does not disrupt the linear extension of sphingosine base of SM. That may well explain why SM is enriched in DRM. It is known that in biomembranes, PC lipids frequently contain a saturated *sn*-1 acyl chain, which can have Chol-inducing condensation effects similar to those of SM (Smaby et al., 1994). Such PC lipids are the most abundant species in DRM (Fridriksson et al, 1999), which is consistent with our ESR evidence that these membranes contain liquid ordered structures. Chol has a stronger condensing effect on SM monolayers than on PC monolayers (Lund-Katz et al., 1988). However, this difference, compared with the strong interactions between the saturated acyl chains and Chol, is a secondary effect. Therefore, if the concentrations of Chol in biomembranes is high enough, strong attractive interactions between Chol and lipids would organize them into DRM domains, with the Chol playing an essential role. Thus we infer that other cell membranes containing high concentrations of Chol should also have a liquid ordered phase. Erythrocyte membranes might be such a case. It was reported that erythrocyte membranes remain fluid at -5°C (Maraviglia et al., 1982), and no gel-to-liquid crystalline phase transition could be detected between -5° and 45°C (Davis et al., 1979).

DRM vesicles have an inhomogeneous structure

One feature of the spectra from 16PC and 5PC in DRM vesicles is that they consist of two components, a normal

three hyperfine line spectrum and a broad single-line spectrum. The latter is likely to be caused by spin exchange interactions due to clustering of nitroxide radicals (Fajer et al., 1992; Earle et al., 1994). Our NLLS analyses showed that ~70% of 5PC and of 16PC molecules partition into an environment of the bilayers where they are enriched. Using a simple model analysis (Earle et al., 1994), we find that they collide with each other at a frequency of $\sim 3 \times 10^8\ s^{-1}$. We are able to discount the possibility that these are micelles (or vesicles) formed by pure 16PC molecules that have separated from the DRM, because the solubility of 16PC in lipid/Chol vesicles is very large: we have prepared a variety of model membrane vesicles containing as much as 5 mol% 16PC (10 times greater than the concentration in the model membranes used in the present experiments). These show exchange broadening characteristic of a single component that is different from what is observed in the present study (see Figs. 2 and 5). Indeed, we find that concentrations of 16PC significantly greater than 5 mol% may be incorporated into model membranes. Our results imply that the model membranes are homogeneous, whereas the DRM vesicles are not.

On the other hand, the spectra from SD-Tempo in DRM vesicles between −5°C and 45°C and the CSL in DRM vesicles we studied (cf. Table 2) can be satisfactorily simulated with only one component. This might suggest that the SD-Tempo (related to SM) and CSL (related to Chol) remain preferentially in the liquid ordered region of the membrane as compared to the PC labels.

The inhomogeneity in DRM could originate from lipid/lipid as well as from lipid/protein interactions. It was reported that heterogeneity of bilayers was induced in bilayers containing gramicidin or bacteriorhodopsin (Williams et al., 1990). The inhomogeneity in the DRM structure could play an important role in the signaling mediated by the IgE receptor and other receptors. Lateral heterogeneity in bilayers has been shown to be important for the function of certain enzymes such as phospholipase A_2 (Hoenger et al., 1996) and protein kinase C (Dibble et al., 1996), and these enzymes are important downstream signaling molecules in IgE receptor-mediated cell activation (Beaven and Metzger, 1993).

CONCLUSIONS

Our ESR study demonstrated that DRM vesicles derived from RBL-2H3 cells have a liquid ordered phase, which is characterized by a liquid-like mobility in both the acyl chain and headgroup regions, and a gel-like ordering in the acyl chain region. This is the first direct evidence that DRMs isolated from live cells have a liquid ordered phase. We also found evidence that DRM vesicles are inhomogeneous, with a second region in which the acyl-chain spin labels are concentrated. This work shows the utility and power of spin-label ESR, especially when combined with quantification by NLLS fitting to the slow motional theory for ESR, in the study of the dynamic structure of biological membranes. It will be interesting to extend these investigations to the plasma membranes of RBL-2H3 cells, to further address the relationship between the structure of DRM domains derived from them and their functional role in the IgE receptor signaling process.

We appreciate helpful discussions with Dr. Erin Sheets. Computations were performed at the Cornell Theory Center and the Cornell Material Science Center.

This work was supported by National Institutes of Health grants GM25862 and AI18306.

REFERENCES

Ahmed, S. N., D. A. Brown, and E. London. 1997. On the origin of sphingolipid/cholesterol-rich detergent-insoluble cell membranes: physiological concentrations of cholesterol and sphingolipids induce formation of a detergent-insoluble, liquid-ordered lipid phase in model membranes. *Biochemistry.* 36:10944–10953.

Anderson, R. G. W. 1998. The caveolae membrane system. *Annu. Rev. Biochem.* 67:199–225.

Beaven, M. A., and H. Metzger. 1993. Signal transduction by receptors: the FcεRI case. *Immunol. Today.* 14:222–226.

Bittman, R., C. R. Kasireddy, P. Mattjus, and J. P. Slotte. 1994. Interaction of cholesterol with sphingomyelin in monolayers and vesicles. *Biochemistry.* 33:11776–11781.

Bloom, M., E. Evans, and O. G. Mouritsen. 1991. Physical properties of the fluid lipid-bilayer component of cell membranes: a perspective. *Q. Rev. Biophys.* 24:293–397.

Brown, D. A., and E. London. 1998a. Functions of lipid rafts in biological membranes. *Annu. Rev. Cell Dev. Biol.* 14:111–136.

Brown, D. A., and E. London. 1998b. Structure and origin of ordered lipid domains in biological membranes. *J. Membr. Biol.* 164:103–114.

Brown, D. A., and J. K. Rose. 1992. Sorting of GPI-anchored proteins to glycolipid-enriched membrane subdomains during transport to the apical cell surface. *Cell.* 68:533–544.

Budil, D. E., S. Lee, S. Saxena, and J. H. Freed. 1996. Nonlinear-least-squares analysis of slow-motion EPR spectra in one and two dimensions using a modified Levenberg-Marquardt algorithm. *J. Magn. Reson.* A120:155–189.

Davis, J. H., B. Baraviglia, G. Weeks, and D. V. Godin. 1979. Bilayer rigidity of the erythrocyte membrane ^{2}H-NMR of a perdeuterated palmitic acid probe. *Biochim. Biophys. Acta.* 550:362–366.

Dibble, A. R. G., A. Hinderliter, J. J. Sando, and R. L. Biltonen. 1996. Lipid lateral heterogeneity within phosphatidylcholine/phosphatidylserine/diaylerol vesicles and its influence on protein kinase C activation. *Biophys. J.* 71:1877–1890.

Earle, K. A., J. K. Moscicki, M. Ge, D. E. Budil, and J. H. Freed. 1994. 250 GHz-ESR studies of polarity gradients along the aliphatic chains in phospholipid membranes. *Biophys. J.* 66:1213–1221.

Fajer, P., A. Watts, and D. Marsh. 1992. Saturation transfer, continuous wave saturation, and saturation recovery electron spin resonance studies of chain-spin labeled phosphatidylcholines in the low temperature phases of dipalmitoyl phosphatidylcholine. *Biophys. J.* 61:879–891.

Ferroretto, A., M. Pitto, P. Palestini, and M. Masserini. 1997. Lipid domains in the membrane: thermotropic properties of sphingomyelin vesicles containing GM1 and cholesterol. *Biochemistry.* 36:9232–9236.

Field, K. A., D. Holowka, and B. Baird. 1995. FcεRI-mediated recruitment of p53/56^{lyn} to detergent-resistant membrane domains accompanies cellular signaling. *Proc. Natl. Acad. Sci. USA.* 92:9201–9205.

Field, K. A., D. Holowka, and B. Baird. 1997. Compartmentalized activation of the high affinity immunoglobulin E receptor within membrane domains. *J. Biol. Chem.* 272:4276–4280.

Freed, J. H. 1994. Field gradient ESR and molecular diffusion in model membranes. *Annu. Rev. Biophys. Biomol. Struct.* 23:1–25.

Fridriksson, E. K., P. A. Shipkova, E. D. Sheets, D. Holowka, B. Baird, F. W. McLafferty. 1999. Quantitative analysis of phospholipids in mast cells using tandem high-resolution mass spectrometry. *Biochemistry.* In press.

Ge, M., D. E. Budil, and J. H. Freed. 1994. ESR studies of spin-labeled membranes aligned by isopotential spin-dry ultracentrifugation: lipid-protein interactions. *Biophys. J.* 67:2326–2344.

Ge, M., and J. H. Freed. 1998. Polarity profiles in oriented and dispersed phosphatidylcholine bilayers are different. An ESR study. *Biophys. J.* 74:910–917.

Gennis, R. B. 1989. Biomembranes. Molecular Structure and Function. Springer-Verlag, New York.

Hanada, K., M. Nishijima, Y. Akamatsu, and R. E. Pagano. 1995. Both sphingomyelin and cholesterol participate in the detergent insolubility of alkaline phosphatase, a glycosylphosphatidylinositol anchored protein, in mammalian membranes. *J. Biol. Chem.* 270:6254–6260.

Henze, R. 1980. Dielectric relaxation in lecithin/cholesterol/water mixtures. *Chem. Phys. Lipids.* 27:165–175.

Hoenger, T., K. Jorgensen, R. L. Biltonen, and O. G. Mouritsen. 1996. Correlation between phospholipase A_2 activity and dynamic lipid bilayer micro-heterogeneity. *Biochemistry.* 35:9003–9006.

Huang, J., J. T. Buboltz, and G. W. Feigenson. 1999. Maximum solubility of cholesterol in phosphatidylcholine and phosphatidylethanolamine bilayers. *Biochim. Biophys. Acta.* 1417:89–100.

Ipsen, J. H., G. Karlström, O. G. Mouritsen, H. Wennerström, and M. J. Zuckermann. 1987. Phase equilibria in the phosphatidylcholine-cholesterol system. *Biochim. Biophys. Acta.* 905:162–172.

Jacobs, R., and E. Oldfield. 1979. Deuterium nuclear magnetic resonance investigation of dimyristoyllecithin-dipalmitoyllecithin and dimyristoyllecithin-cholesterol mixtures. *Biochemistry.* 18:3280–3285.

Kar, L., E. Ney-Igner, and J. H. Freed. 1985. Electron spin resonance and electron-spin-echo study of oriented multilayers of L_α-dipalmitoylphosphatidylcholine water system. *Biophys. J.* 48:569–595.

Lewis, R. N. A. H., and R. A. McElhaney. 1991. The mesomorphic phase behavior of lipid bilayers. *In* The Structure of Biological Membranes. P. Yeagle, editor. CRC Press, Boca Raton, FL. 73–155.

Lund-Katz, S., H. M. Laboda, L. R. McLean, and M. C. Phillips. 1988. Influence of molecular packing and phospholipid type on rates of cholesterol exchange. *Biochemistry.* 27:3416–3423.

Maraviglia, B., J. H. Davis, M. Bloom, J. Westerman, and K. W. A. Wirtz. 1982. Human erythrocyte membranes are fluid down to −5°C. *Biochim. Biophys. Acta.* 686:137–140.

Marsh, D. 1990. Handbook of Lipid Bilayers. CRC Press, Boca Raton, FL.

McIntosh, T. J. 1978. The effect of cholesterol on the structure of dipalmitoylphosphatidylcholine. *Biochim. Biophys. Acta.* 513:43–58.

McIntosh, T. J., A. D. Magid, and S. A. Simon. 1989. Cholesterol modifies the short-range repulsive interactions between phosphatidylcholine membranes. *Biochemistry.* 28:17–25.

Meirovitch, E., D. Igner, G. Moro, and J. H. Freed. 1982. Electron-spin relaxation and ordering in smectic and supercooled nematic liquid crystals. *J. Chem. Phys.* 77:3915–3938.

Meirovitch, E., A. Nayeem, and J. H. Freed. 1984. Analysis of protein-lipid interactions based on model simulations of electron spin resonance spectra. *J. Phys. Chem.* 88:3454–3465.

Needham, D., T. J. McIntosh, and E. Evans. 1988. Thermomechanical and transition properties of dimyristoylphosphatidylcholine/cholesterol bilayers. *Biochemistry.* 27:4668–4673.

Pierini, L., D. Holowka, and B. Baird. 1996. FcεRI-mediated association of 6-μm beads with RBL-2H3 mast cells results in exclusion of signaling proteins from the forming phagosome and abrogation of normal downstream signaling. *J. Cell Biol.* 134:1427–1439.

Rubenstein, J. L. R., B. A. Smith, and H. M. McConnell. 1979. Lateral diffusion in binary mixtures of cholesterol and phosphatidylcholines. *Proc. Natl. Acad. Sci. USA.* 76:15–18.

Schneider, D. J., and J. H. Freed. 1989. Calculating slow motional magnetic resonance spectra: a user's guide. *In* Spin Labeling Theory and Applications, Vol. 8. L. J. Berliner and J. Reuben, editors. Plenum Press, New York. 1–76.

Schroeder, R., S. N. Ahmed, Y. Zhu, E. London, and D. A. Brown. 1998. Cholesterol and sphingolipid enhance the Triton X-100-insolubility of GPI-anchored proteins by promoting the formation of detergent-insoluble ordered membrane domains. *J. Biol. Chem.* 273:1150–1157.

Schroeder, R., E. London, and D. A. Brown. 1994. Interactions between saturated acyl chains confer detergent resistance on lipids and glycosylphosphatidylinositol (GPI)-anchored proteins: GPI-anchored proteins in liposomes and cells show similar behavior. *Proc. Natl. Acad. Sci. USA.* 91:12130–12134.

Sheets, E. D., D. Holowka, and B. Baird. 1999. Membrane organization in IgE receptor signaling. *Curr. Opin. Chem. Biol.* 3:95–99.

Shin, Y.-K., and J. H. Freed. 1989a. Dynamic imagine of lateral diffusion by electron spin resonance and study of rotational dynamics in model membranes. Effect of cholesterol. *Biophys. J.* 55:537–550.

Shin, Y.-K., and J. H. Freed. 1989b. Thermodynamics of phosphatidylcholine-cholesterol mixed model membranes in the liquid crystalline state studied by the orientational order parameter. *Biophys. J.* 56:1093–1100.

Simons, K., and E. Ikonen. 1997. Functional rafts in cell membranes. *Nature.* 387:569–572.

Smaby, J. M., H. L. Brockman, and R. E. Brown. 1994. Cholesterol's interfacial interactions with sphingomyelins and phosphatidylcholine: hydrocarbon chain structure determines the magnitude of condensation. *Biochemistry.* 33:9135–9142.

Smaby, J. M., M. Momsen, V. S. Kulkarni, and R. Brown. 1996. Cholesterol-induced interfacial area condensations of galactosylceramides and sphingomyelins with identical acyl chains. *Biochemistry.* 35: 5696–5704.

Straume, M., and B. J. Litman. 1987. Influence of cholesterol on equilibrium and dynamic bilayer structure of unsaturated acyl phosphatidylcholine vesicles as determined from higher order analysis of fluorescence anisotropy decay. *Biochemistry.* 26:5121–5126.

Tanaka, H., and J. H. Freed. 1984. Electron spin resonance studies on ordering and rotational diffusion in oriented phosphatidylcholine multilayers: evidence for a new chain-ordering transition. *J. Phys. Chem.* 88:6633–6643.

Tanaka, H., H. Saito, and H. Kawazura. 1997. Use of $VO^{2+}S$ as a spin label for dynamics of polar headgroups in phosphatidylcholine bilayers. *Chem. Phys. Lipids.* 85:45–51.

Vist, M. R., and J. H. Davis. 1990. Phase equilibria of cholesterol/dipalmitoylphosphatidylcholine mixtures: ^{2}H nuclear magnetic resonance and differential scanning calometry. *Biochemistry.* 29:451–464.

Williams, B. W., A. W. Scotto, and C. D. Stubbs. 1990. Effect of proteins on fluorophore lifetime heterogeneity in lipid bilayers. *Biochemistry.* 29:3248–3255.

Yeagle, P. L., W. C. Hutton, and R. B. Martin. 1975. Head group conformation and lipid-cholesterol association in phosphatidylcholine vesicles: a ^{31}P (^{1}H) nuclear Overhauser effect study. *Proc. Natl. Acad. Sci. USA.* 72:3477–3481.

Yeagle, P. L., W. C. Hutton, C.-H. Huang, and R. B. Martin. 1977. Phospholipid head-group conformations: intermolecular interactions and cholesterol effects. *Biochemistry.* 16:4344–4349.